Article

Cell Reports

Group 2 Innate Lymphoid Cells Attenuate Inflammatory Arthritis and Protect from Bone Destruction in Mice

Graphical Abstract

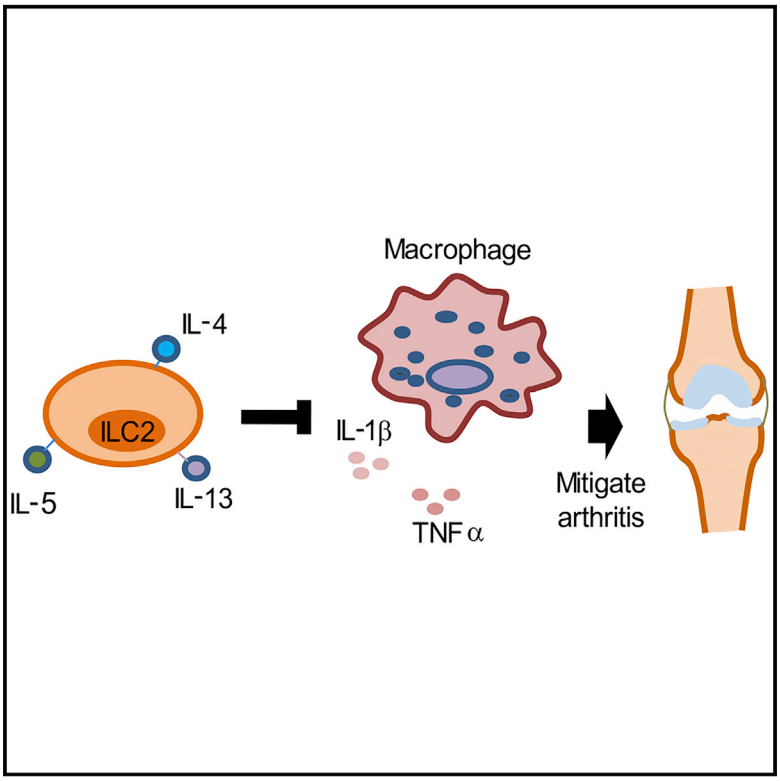

Authors

Yasunori Omata, Michael Frech, Tatjana Primbs, ..., Stefan Wirtz, Georg Schett, Mario M. Zaiss

Correspondence

mario.zaiss@uk-erlangen.de

In Brief

The role of ILC2s in the initiation phase of inflammatory arthritis has remained unclear. Omata et al. demonstrate that the ILC2-derived IL-4/13 decrease pro-inflammatory cytokine secretion by macrophages, thereby attenuating arthritis.

Highlights

- ILC2s in RA are increased in blood and synovial tissue compared with healthy controls
- ILC2s in RA inversely correlate with disease activity
- Artificially elevated ILC2 levels significantly attenuated arthritis in animal models
- ILC2s attenuated arthritis in an IL-4/13-dependent manner

Omata et al., 2018, Cell Reports *24*, 169–180
July 3, 2018
https://doi.org/10.1016/j.celrep.2018.06.005

CellPress

Cell Reports
Article

Group 2 Innate Lymphoid Cells Attenuate Inflammatory Arthritis and Protect from Bone Destruction in Mice

Yasunori Omata,[1] Michael Frech,[1] Tatjana Primbs,[2] Sébastien Lucas,[1] Darja Andreev,[1] Carina Scholtysek,[1] Kerstin Sarter,[1] Markus Kindermann,[2] Nataliya Yeremenko,[3] Dominique L. Baeten,[3] Nico Andreas,[4] Thomas Kamradt,[4] Aline Bozec,[1] Andreas Ramming,[1] Gerhard Krönke,[1] Stefan Wirtz,[2] Georg Schett,[1] and Mario M. Zaiss[1,5,*]

[1]Department of Internal Medicine 3, Rheumatology and Immunology, Friedrich-Alexander-University Erlangen-Nürnberg (FAU) and Universitätsklinikum Erlangen, Erlangen, Germany

[2]Department of Internal Medicine 1, University of Erlangen-Nuremberg, Erlangen, Germany

[3]Department of Clinical Immunology and Rheumatology and Department of Experimental Immunology, Academic Medical Center/University of Amsterdam, Amsterdam, the Netherlands

[4]Institute of Immunology, Jena University Hospital, Leutragraben 3, 07743 Jena, Germany

[5]Lead Contact

*Correspondence: mario.zaiss@uk-erlangen.de

https://doi.org/10.1016/j.celrep.2018.06.005

SUMMARY

Group 2 innate lymphoid cells (ILC2s) were detected in the peripheral blood and the joints of rheumatoid arthritis (RA) patients, serum-induced arthritis (SIA), and collagen-induced arthritis (CIA) using flow cytometry. Circulating ILC2s were significantly increased in RA patients compared with healthy controls and inversely correlated with disease activity. Induction of arthritis in mice led to a fast increase in ILC2 number. To elucidate the role of ILC2 in arthritis, loss- and gain-of-function mouse models for ILC2 were subjected to arthritis. Reduction of ILC2 numbers in *RORα^{cre}/GATA3$^{fl/fl}$* and *Tie2^{cre}/ROR$\alpha^{fl/fl}$* mice significantly exacerbated arthritis. Increasing ILC2 numbers in mice by IL-25/IL-33 mini-circles or IL-2/IL-2 antibody complex and the adoptive transfer of wild-type (WT) ILC2s significantly attenuated arthritis by affecting the initiation phase. In addition, adoptive transfer of IL-4/13-competent WT but not *IL-4/13$^{-/-}$* ILC2s and decreased cytokine secretion by macrophages. These data show that ILC2s have immune-regulatory functions in arthritis.

INTRODUCTION

Innate lymphoid cells (ILCs) are rare immune cells defined by their lack of T cell receptors and absence of lineage markers. Nevertheless, they share many functional similarities with T cells. Although T cells outnumber ILCs by far, ILCs are often the first responders, initiating critical immune responses before adaptive immunity starts. ILCs may therefore play a role in the initiation of arthritis, but functional data on ILCs in arthritis are limited to date. Recent work suggested that a specific form of ILCs, ILC3s, which are a source of IL-17 and IL-22, reside in entheses and are enriched in the joints of patients with spondyloarthritis (Ciccia et al., 2012, 2015; Cuthbert et al., 2017; Leijten et al., 2015). Some analyses have also been carried out in rheumatoid arthritis (RA) patients showing that ILC1 and ILC3 reside in the synovial fluid of RA patients (Dalbeth and Callan, 2002; Koo et al., 2013; Ren et al., 2011) and are positively correlated with clinical disease activity (Koo et al., 2013). In one study of subjects with pre-clinical RA, in which the authors did not distinguish between ILC1 and ILC2, the combined ILC1/2 population presented a larger proportion of ILCs in lymph nodes compared with healthy controls, suggesting that ILCs may be involved in RA from the very beginning (Rodríguez-Carrio et al., 2017). Apart from these descriptive studies on ILC1 and ILC3, data on the function of ILCs in RA are rare. Recently, we showed that ILC2s induce the resolution of arthritis via the production of IL-9, which in turn restores the suppressive capacity of Tregs, enabling them to suppress chronic inflammation (Rauber et al., 2017). In this context, studies of ILC2s are highly interesting, as they are linked to Th2 cell activation, which has recently been described as a regulatory pathway in RA (Chen et al., 2016).

In this study we addressed the role of ILC2s in the initiation phase of RA. On the basis of the cytokine signature and the induction of type 2 immune responses that lead to enhanced tissue repair, along with control of inflammation (Chen et al., 2016; Gause et al., 2013), we hypothesized that ILC2s have an attenuating effect on RA. To test this concept, we investigated different ILC2 gain- and loss-of-function models during inflammatory arthritis. We could show that ILC2 numbers are increased both in RA patients and in inflammatory arthritis mouse models. In two settings of genetically reduced ILC2 numbers, arthritis was exacerbated, while therapeutic enhancement of ILC2 numbers significantly attenuated arthritis. This regulatory action of ILC2s was dependent on their capacity to secret IL-4/13, as *IL4/13$^{-/-}$* ILC2s failed to attenuate arthritis after adoptive cell transfer. Mechanistically, ILC2-derived IL-4/13 significantly suppressed IL-1β section by macrophages, and it was shown that both IL-1β and macrophages are key players driving early clinical symptoms in SIA and RA (Ji et al., 2002; Misharin et al., 2014). This mechanism was critical only during the initiation phase of

arthritis, as therapeutically adoptive ILC2 transfer at later time points also failed to attenuate arthritis. Our data thus reveal essential regulatory functions of ILC2s in inflammatory arthritis.

RESULTS

ILC2s Are Increased in RA Patients and Inversely Correlate with Disease Activity

We first assessed ILC2 numbers in peripheral blood samples from RA patients and healthy controls using flow cytometry. ILC2s were identified as lineage-negative (CD3, CD11c, CD123, CD14, CD34, TCR$\alpha\beta$, TCR$\gamma\delta$, CD303, and CD94) CD127$^+$ CD161$^+$ CRTH$^+$ GATA3$^+$ cells. Although circulating ILC2s were low in healthy controls, their relative and absolute numbers were elevated in RA patients (Figure 1A). When analyzing RA patients, who had elevated ILC2s (>0.7% of leukocytes), ILC2s were inversely correlated to disease activity as measured by DAS28-ESR scores (Figure 1B). Furthermore, when comparing RA patients with inactive (DAS28-ESR < 3.2) versus active (DAS28-ESR $\geq$ 3.2) disease, ILC2s were significantly higher in RA patients with inactive disease (Figure 1B). Of note, ILC2s were also detected in the synovial tissue of RA patients with a tendency toward elevated numbers compared with peripheral blood samples taken from the same patients (Figure 1C). Hence, the observed increase in RA patients together with their presence in the synovial tissue highlights their possible systemic as well as local involvement during RA.

ILC2s Are Induced during Experimental Arthritis and Primarily Secrete IL-4

Next, two different arthritis mouse models, namely the K/BxN serum transfer (SIA; passive transfer of antibodies) and the collagen-induced arthritis (CIA) model (active immunization with chicken collagen type II followed by collagen boost injection 21 days later), were analyzed for the dynamics of ILC2 regulation during arthritis. ILC2 numbers, identified as lineage-negative (CD3ε, CD4, CD8a, CD11b, and CD16l) CD90.2$^+$ KLRG1$^+$ ST2$^+$ GATA3$^+$, rapidly increased after disease onset in SIA (Figure 1D) and CIA (Figure 1E). Along with the initiation phase of arthritis IL-4-competent ILC2s accounted for the most significant proportion of ILC2s, followed by IL-5-competent and IL-13-competent ILC2 in descending order (Figures 1D and 1E). Although we observed a significant increase of ILC2s in the SIA model, only Th1 (CD4$^+$ T-bet$^+$) cells increased at a comparable rate, whereas Th2 (CD4$^+$ GATA3$^+$), Th17 (CD4$^+$ RORγt$^+$), and Tregs (CD4$^+$ Foxp3$^+$) were not significantly changed (Figure 1F).

To further confirm the presence of ILC2s in the inflamed joints, we analyzed synovial tissue using fluorescence-activated cell sorting (FACS) and could show that ILC2s can be found in the blood and the synovial tissues when clinical signs of arthritis were fully developed at 8 days post-SIA induction (Figure 1G). In the bone marrow, where ILC2s develop from their progenitors, IL-4-competent ILC2s were significantly upregulated and accounted for more than 80% of total ILC2s already on day 4 post-SIA induction (Figure 1H). Interestingly, their numbers in synovial tissue increased at later time points, at 8 days post-SIA induction (Figure 1H), possibly showing their early accumulation in the bone marrow, followed by their later egress to the synovial tissue. Also, we investigated ILC2s immunohistochemically at 8 days post-SIA induction in the inflamed joints by using bone marrow chimeras with *Rorα^{cre} TdTomato$^{fl/fl}$* reporter as donor mice and wild-type as recipient mice (to reduce the strong fluorescence of radio-resistant cells in the *Rorα^{cre} TdTomato$^{fl/fl}$* mice) after SIA induction. There, we could show the presence of ILC2s, identified according to the expression of *RORa* as the essential transcription factor besides *GATA3* (Halim et al., 2012; Mjösberg et al., 2012) in combination with IL-17RB in the inflamed arthritic tarsal joints of the hind paws (Figure 1I). These results show that similar to RA patients, ILC2s are upregulated in two different arthritis mouse models both systemically and locally in the inflamed joints.

Reduced ILC2 Numbers in Mice Exacerbate Arthritis and Bone Destruction

To examine the functional role of ILC2s, we investigated two independent mice strains showing genetically reduced ILC2 numbers, namely *Rora^{cre}Gata3$^{fl/fl}$* (Figures 2A–2F) and *Tie2^{cre}/Ror$\alpha^{fl/fl}$* mice (Figures 2G–2L). First, *Rora^{cre}Gata3$^{fl/fl}$* mice showed higher arthritic scores after induction of SIA compared with littermate control mice *Rora^{cre}Gata3$^{wt/wt}$* (wild-type [WT]) (Figure 2B). Exacerbated arthritis scores in *Rora^{cre}Gata3$^{fl/fl}$* were associated with increased bone erosions and inflamed areas in the affected paws analyzed by histomorphometry (Figures 2C and 2D). Systemically, *Rora^{cre}Gata3$^{fl/fl}$* mice showed no obvious difference in systemic bone mass, presented as bone volume per total volume (BV/TV), but significant upregulated osteoclast numbers (Figure 2E). In addition, there was no difference in Th17 and Treg numbers (Figure 2F) and T cell-derived serum cytokine levels, except for reduced IL-22 serum concentrations (Figure S1A), while a significant increase in CD11b$^+$F4/80$^+$ macrophages, a well described source of pro-inflammatory cytokines like IL-1β, was detected (Figure 2G).

Also *Tie2^{cre}/Ror$\alpha^{fl/fl}$* mice showed exacerbated arthritis after SIA induction compared to littermate *Tie2^{cre}/Ror$\alpha^{wt/wt}$* (WT) control mice (Figures 2H and S2A) along with significantly reduced ILC2 numbers (Figures 2I and 2J). Of note, among the analyzed cytokines secreted by ILC2s in *Tie2^{cre}/Ror$\alpha^{fl/fl}$* mice, IL-4, together with IL-5, were the most prominent ones when detected by intracellular FACS analysis (Figure 2I). To investigate if other lymphocyte subsets or cytokines are involved, we analyzed Treg, Th1, Th2 and Th17 cell populations and T cell-derived cytokines and could not detect any differences at day 8 post-SIA induction (Figures 2K, 2L, and S1B). These data support a functional role of ILC2s in arthritis, which is related to immune regulation rather than activation, as two mice strains with genetically reduced ILC2 numbers showed exacerbated clinical arthritis.

Systemic *In Vivo* Induction of ILC2s Attenuate Arthritis and Bone Destruction

IL-25 and IL-33 were shown to elicit ILC2s (Fallon et al., 2006; Moro et al., 2010; Neill et al., 2010; Salimi et al., 2013), and recently a role of IL-33 in the egress of ILC2s from the bone marrow has been reported (Stier et al., 2018). Therefore, we used the mini-circle (mc) technology (Liu et al., 1999; McHedlidze et al., 2013) to systemically overexpress IL-25 and IL-33 (Figure S2B) in order to analyze if increased ILC2 numbers

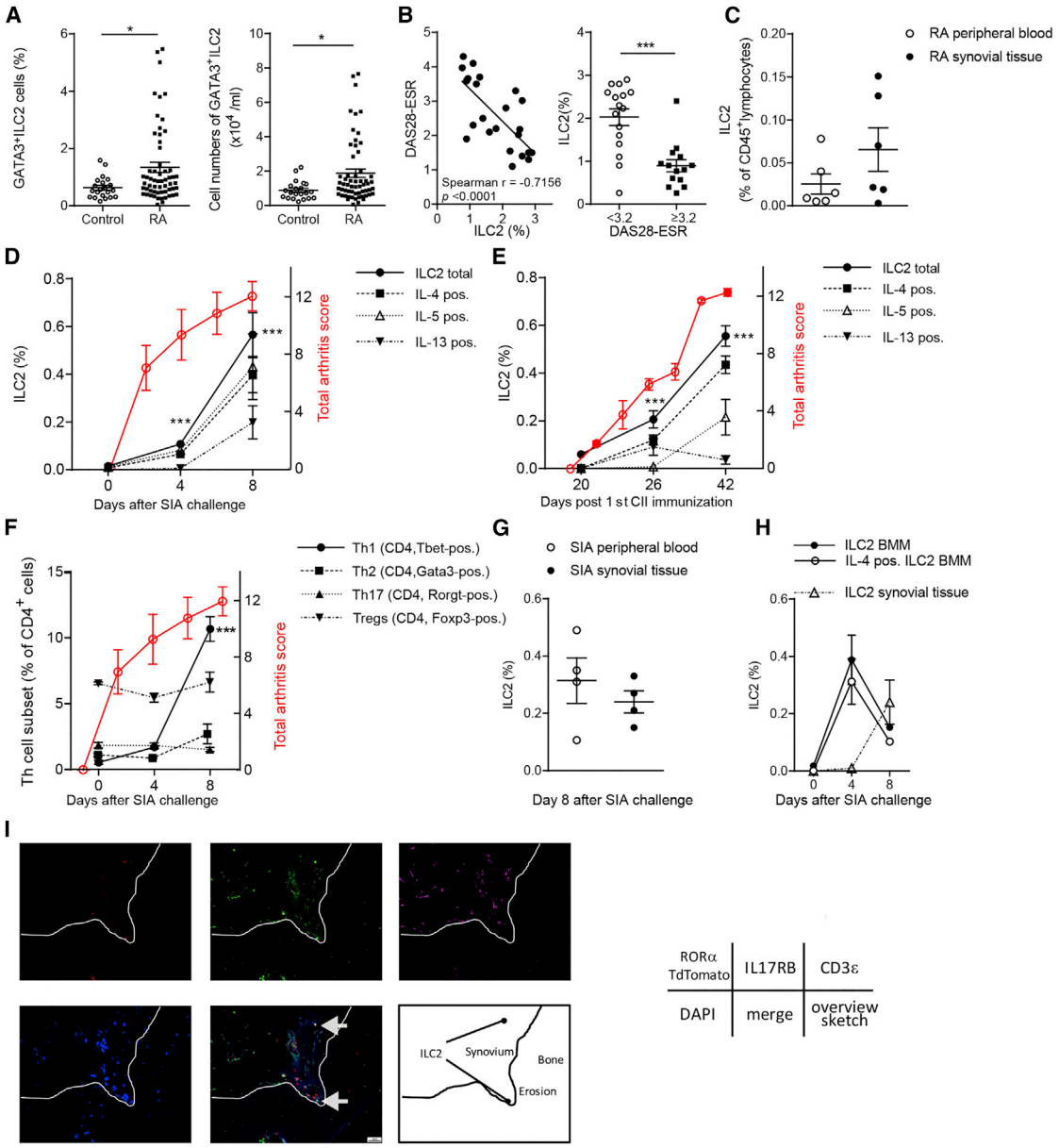

Figure 1. Group 2 Innate Lymphoid Cells Are Increased in Rheumatoid Arthritis Patients and Inflammatory Arthritis Models

(A) Flow cytometry analysis of GATA3$^+$ ILC2s in the peripheral blood. ILC2s identified as lineage-negative (CD3, CD11c, CD14, CD19, CD34, CD123, TCRαβ, TCRγδ, CD303, FceR1, and CD94) CD127$^+$ CD161$^+$ CRTH$^+$ and GATA3$^+$ cells in healthy controls (n = 21) and RA (n = 59) patients. Shown as percentages in total cells (left) and absolute numbers per milliliter (right).

(B) Left: correlation plot between ILC2 and disease activity demonstrated by disease activity score 28 (DAS28) based on erythrocyte sedimentation rate (ESR) in RA patients with elevated ILC2s. Right: ILC2 numbers in inactive (DAS28-ESR < 3.2) and active (DAS28-ESR ≥ 3.2) RA patients.

(C) ILC2 numbers in human peripheral blood and human synovial tissue from the same patients.

(D) ILC2s in serum-induced arthritis (SIA) and (E) collagen-induced arthritis (CIA). Flow cytometry analysis of ILC2s in the spleen identified as lineage-negative (CD3e, CD4, CD8a, CD19, CD11b, and CD161) CD45$^+$, CD90.2$^+$, ST2$^+$, KLRG1$^+$, GATA3$^+$ cells, with additional intracellular staining for IL-4, IL-5, and IL-13 expression. Results are representative of two independent experiments.

(F) Flow cytometry analysis of splenic Th cell subsets in SIA.

(G) Comparison of ILC2 numbers in the peripheral blood and synovial tissues in SIA.

(H) Flow cytometry analysis of ILC2s in the bone marrow and synovial tissue in SIA.

(I) Immunohistological detection of ILC2s in the joints of wild-type irradiated recipient mice transferred with *Rora^{cre} TdTomato$^{fl/fl}$* bone marrow donor mice and induced for SIA.

Representative data are from one of two independent experiments. Data are expressed as mean ± SEM. *p < 0.05 and ***p < 0.001. Statistical analyses were performed by comparing against control or day 0 samples in each analysis group.

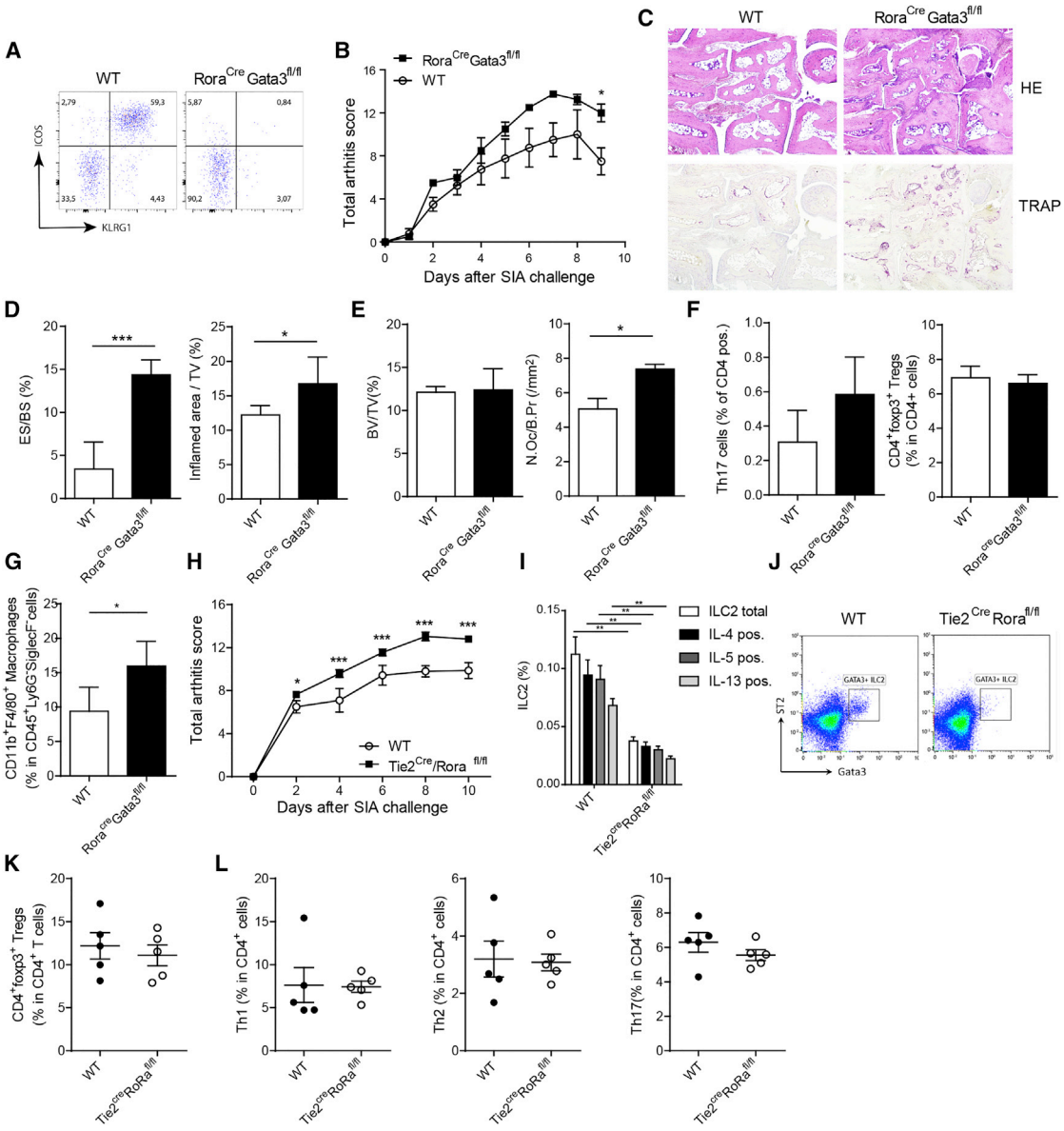

Figure 2. Exacerbation of Arthritis in *Rora^{cre}Gata3$^{fl/fl}$* and *Tie2^{Cre}Rora $^{fl/fl}$* Mice with Reduced ILC2 Numbers

(A–G) SIA was induced in *Rora^{cre}Gata3$^{fl/fl}$* and littermate control *Rora^{cre}Gata3$^{wt/wt}$* (wild-type [WT]) mice. Samples were obtained at day 9 after induction of SIA.

(A) Representative FACS plot of the lung cells to illustrate genetic reduction of ILC2s in *Rora^{cre}Gata3$^{fl/fl}$* mice.

(B) Arthritis scores in WT littermates and *Rora^{cre}Gata3$^{fl/fl}$* mice (SIA) (n = 5).

(C) Representative H&E and tartrate-resistant acid phosphatase (TRAP) stains of tarsal joints of hind paw sections of the two genotypes.

(D) Histomorphological analysis of paws showing eroded surface per bone surface (ES/BS) and inflamed area per total volume (TV).

(E) Systemic bone volume per tissue volume (BV/TV) and osteoclast number per bone perimeter (OcN/B.Pm) in the tibias of respective mice.

(F and G) Flow cytometry of spleen cells for Th17 and CD4$^+$foxp3$^+$Treg number (F) and CD11b$^+$F4/80$^+$ macrophage number (G).

(H–L) SIA was induced in *Tie2^{Cre}Rora $^{fl/fl}$* and littermate *Tie2^{cre}/Ror$\alpha^{wt/wt}$* (WT) control mice.

(H) Arthritis scores in WT littermates and *Tie2^{Cre}Rora $^{fl/fl}$* mice (n = 5).

(I) Total ILC2s and IL-4/IL-5/IL-13 expressing ILC2 numbers in the spleen at day 10 after induction of SIA.

(J) Representative FACS plot of the spleen cells to illustrate genetic reduction of ILC2s in *Tie2^{cre} ROR$\alpha^{fl/fl}$* mice.

(K and L) Flow cytometry of spleen cells for CD4$^+$foxp3$^+$Tregs (K) and effector Th1/2/17 cell numbers (L).

Representative data are from one of two independent experiments. Data are expressed as mean ± SEM; n = 5. *p < 0.05, **p < 0.01, and ***p < 0.001.

mitigate arthritis. IL-25/33 mc-treated mice showed significantly attenuated arthritis compared with control mice (Figures 3A and S2C), along with systemically increased total ILC2 numbers (Figure 3B). Of note, IL-4- and IL-5-competent ILC2s represented the highest proportion of ILC2s (Figure 3B). Locally, immunohistological and FACS analysis of the paws and the synovial tissues,

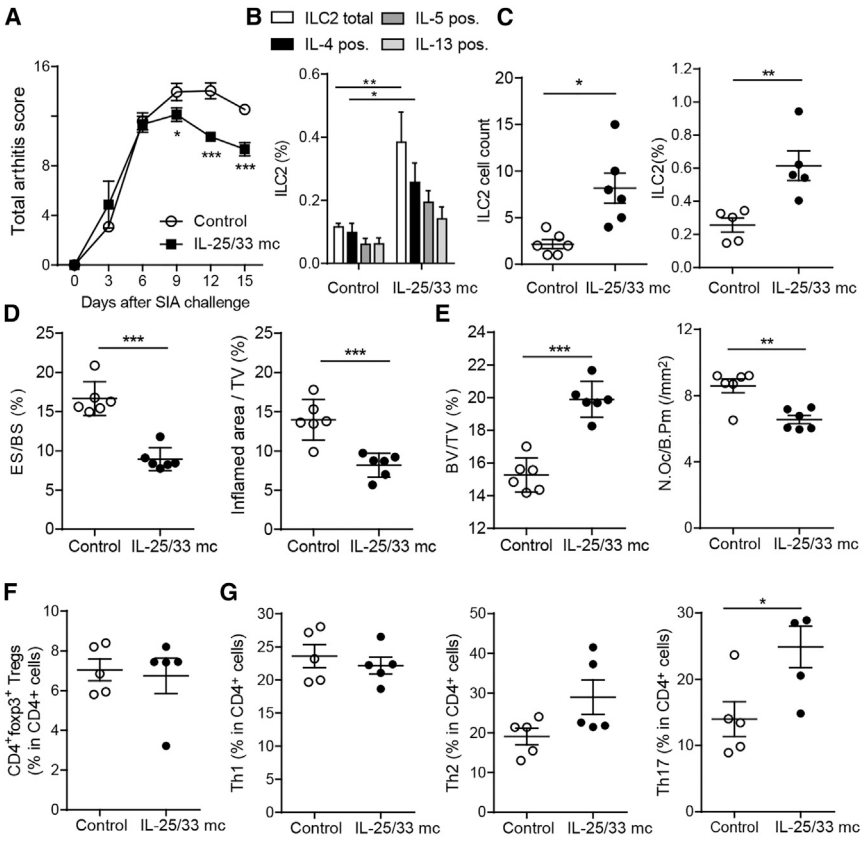

Figure 3. *In Vivo* ILC2 Expansion by Mini-Circle IL-25/-33 Vector Attenuates Arthritis

Expansion of ILC2s by IL-25/33 mc and induction of SIA (n = 6). The samples are obtained at day 14 after induction of SIA.

(A) Arthritis scores in control and IL-25/33 mc-treated mice.

(B) Flow cytometry analysis of total and IL-4$^+$/IL-5$^+$/IL-13$^+$ expressing ILC2s in the spleen. ILC2s identified as lineage-negative (CD3e, CD4, CD8a, CD19, CD11b, and CD161) CD45$^+$, CD90.2$^+$, ST2$^+$, KLRG1$^+$, GATA3$^+$ cells.

(C) Immunohistological analysis of ILC2s in paws (left) and flow cytometry analysis of ILC2s in synovial tissue (right).

(D) Histomorphological analysis of paws showing eroded surface per bone surface (ES/BS) and inflamed area per total volume (TV).

(E) Systemic bone volume per tissue volume (BV/TV) and osteoclast number per bone perimeter (OcN/B.Pm) in the tibias of respective mice.

(F and G) Flow cytometry of spleen cells for CD4$^+$foxp3$^+$Treg (F) and effector Th1/2/17 (G) cell numbers.

Representative data are from one of three independent experiments. Data are expressed as mean ± SEM; n = 5. *p < 0.05, **p < 0.01, and ***p < 0.001.

respectively, showed significantly increased ILC2 numbers following IL-25/33 mc treatment (Figure 3C). Histomorphological analysis of the paws revealed reduced bone erosions along with less inflammation in IL-25/33 mc-treated mice after SIA induction on day 14 (Figure 3D). Also systemically, BV/TV was increased, and osteoclast numbers per analyzed bone surface were reduced in tibial sections (Figure 3E). Analysis of Treg, Th1, and Th2 cells revealed no significant difference, whereas Th17 cells were surprisingly increased in IL-25/33 mc-treated mice at 14 days post-SIA induction (Figures 3F and 3G). Serum cytokines were unchanged (Figure S1C). To further strengthen the regulatory role of ILC2 gain of function during SIA, IL-2/IL-2 antibody complex (IL2c) treatment was used (Pelly et al., 2016). IL2c treatment resulted in significantly attenuated arthritis scores compared with untreated controls (Figures 4A and S2D) as well as significantly increased ILC2 numbers in the spleen (Figure 4B) and locally in the inflamed synovial tissue (Figure 4C). Inflamed areas in the joints (Figure 4D), bone erosions, and osteoclast numbers in the joints (Figure 4E) were reduced upon IL2c treatment, while bone volume was improved, confirming our previous observations in ILC2 induction experiments by IL-25/33 mc treatment. However, in the IL2c-treated mice, we could not observe any significant changes in Treg, Th1, Th2, or Th17 cell populations or serum cytokines (Figures 4F, 4G, and S3A). Of note, IL2c treatment in *Tie2^{cre}/Ror$\alpha^{fl/fl}$* mice failed to attenuate arthritis scores compared with untreated control *Tie2^{cre}/Ror$\alpha^{fl/fl}$* mice (Figure S2E). Although we cannot rule out any other non-investigated cell type being responsible for the observed attenuating effects after *in vivo* ILC2 expansion, these results strongly suggests that ILC2s have a positive role on arthritic disease severity.

Transfer of ILC2s Attenuates Arthritis and Bone Destruction

Furthermore, in order to have direct proof that ILC2s alone can attenuate arthritis, we performed adoptive transfer experiments with sorted and *ex vivo* expanded ILC2s (Duerr et al., 2016) transferred into WT recipient mice before SIA was induced (Figure 5). ILC2 transfer into WT mice significantly reduced arthritis (Figure 5A). We also found systemically increased ILC2 numbers in the spleen, with IL-4-competent ILC2s contributing to more than 60% of total analyzed ILC2s (Figure 5B) as well as locally in the affected, inflamed synovial tissue by FACS analysis (Figure 5C). Similar to the results obtained by systemic induction of ILC2s (Figures 3 and 4), adoptive transfer of ILC2s reduced bone erosions and inflamed areas in the affected paws 14 days after SIA induction (Figure 5D). Even systemically, we observed an increase in BV/TV and a concomitant decrease in osteoclast numbers per analyzed bone surface (Figure 5E). Furthermore, WT ILC2s were adoptively transferred also into *IL-7R$^{-/-}$* recipient mice (Figures 5F–5J), as it was shown that IL-7 is essential for ILC2 differentiation (Moro et al., 2010; Robinette et al., 2017; Vonarbourg and Diefenbach, 2012). The observed anti-arthritic effect after adoptive WT ILC2 transfer into WT recipient mice was even more pronounced in IL-7R$^{-/-}$ recipient mice (Figure 5F). Similar to WT recipient mice, IL-7R$^{-/-}$ recipient mice

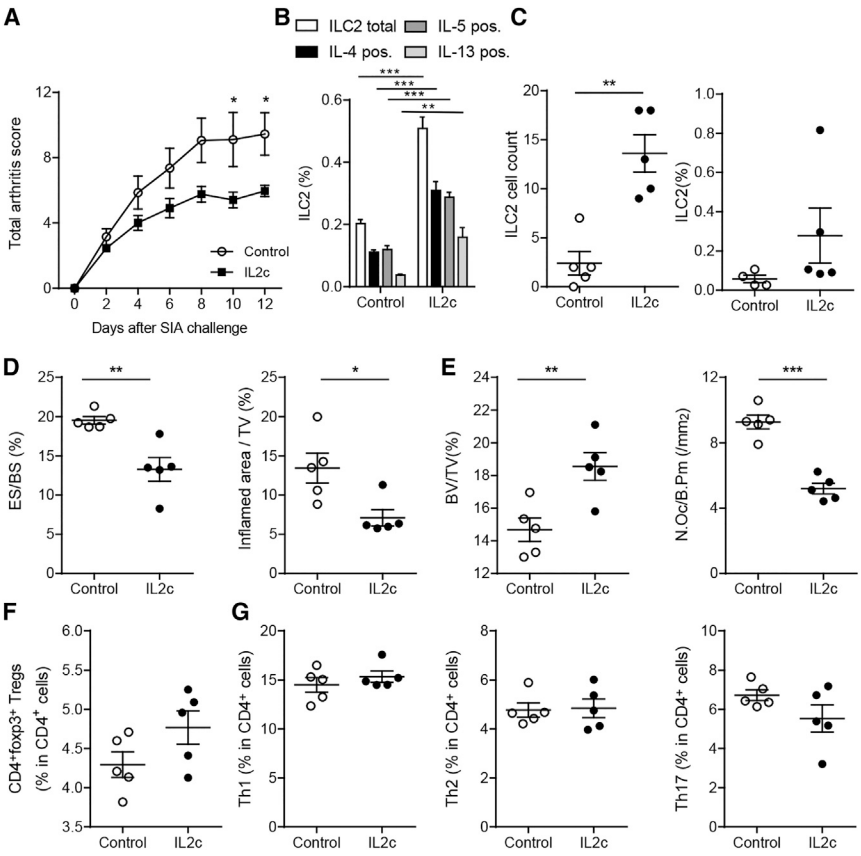

Figure 4. *In Vivo* ILC2 Expansion by IL-2/IL-2 Antibody Complex Attenuates Arthritis

Expansion of innate lymphoid cells 2 (ILC2s) by IL-2/IL-2 antibody complex (IL2c) and induction of SIA (n = 5). The samples are obtained at day 12 after induction of SIA.

(A) Arthritis scores in control and IL-25/33 mc treated mice.

(B) Flow cytometry analysis of total and IL-4$^+$/IL-5$^+$/IL-13$^+$ expressing ILC2s in the spleen. ILC2s identified as lineage-negative (CD3e, CD4, CD8a, CD19, CD11b, and CD161) CD45$^+$, CD90.2$^+$, ST2$^+$, KLRG1$^+$, GATA3$^+$ cells.

(C) Immunohistological analysis of ILC2s in paws (left) and flow cytometry analysis of ILC2s in synovial tissue (right).

(D) Histomorphological analysis of paws showing eroded surface per bone surface (ES/BS) and inflamed area per total volume (TV).

(E) Systemic bone volume per tissue volume (BV/TV) and osteoclast number per bone perimeter (OcN/B.Pm) in the tibias of respective mice.

(F and G) Flow cytometry of spleen cells for CD4$^+$foxp3$^+$Treg (F) and effector Th1/2/17 (G) cell numbers.

Representative data are from one of three independent experiments. Data are expressed as mean ± SEM; n = 5. *p < 0.05, **p < 0.01, and ***p < 0.001.

showed increased ILC2 numbers (Figures 5G and 5H), and decreased inflamed area and bone erosions (Figure 5I) in the affected paws as well as increased systemic BV/TV along with a reduction in osteoclast numbers in the tibia (Figure 5J). Again, as IL-7R$^{-/-}$ are not completely lacking ILC, and IL-7 signaling might affect other potentially important cell types as well, we additionally performed the SIA mouse model in IL-7R$^{-/-}$ mice without adoptively transferred ILC2s. Surprisingly, we observed per se improved clinical arthritis scores (Figures S4A and S4B) but unchanged Treg, Th1, and Th2 immune cells responses, whereas Th17 cells were significantly upregulated in IL-7R$^{-/-}$ mice compared with WT controls (Figures S4C and S4D). Nevertheless, adoptive WT ILC2 transfers further attenuated the observed phenotype in IL-7R$^{-/-}$ mice. These results corroborate that the observed phenotypes after *in vivo* ILC2 expansion were independent of other potential target cells types, as the induction of ILC2s and the adoptive transfer of these cells yielded very similar results.

IL-4/13-Competent ILC2s Are Essential for the Observed Attenuating Effects

Because in our experiments shown so far, IL-4-competent ILC2s represented the highest proportion of total ILC2, we adoptively transferred ILC2 from IL-4/13$^{-/-}$ mice and compared them with WT ILC2s (Figure 6). Interestingly, adoptive transfer of IL-4/13$^{-/-}$ ILC2s did not show significant attenuation of clinical arthritis, whereas WT ILC2s did (Figures 6A and S2F). Again, FACS analysis revealed the successful ILC2 transfer, as both ILC2 recipient groups showed increased ILC2 numbers compared with control group that did not receive ILC2s (Figure 6B). Serum cytokine analysis on day 8 post-SIA induction showed significant upregulated IL-4 concentrations in WT ILC2-transferred recipient mice (Figure 6C). The levels of pro-inflammatory IL-1β and TNFα were reduced, although non-significantly, after transfer of WT ILC2s and even significantly increased after IL-4/13$^{-/-}$ ILC2 transfer (Figure 6D). Other investigated effector serum cytokines, except IL-6 at day 4, remained unchanged at day 4 and day 8 post-SIA induction (Figures S3B and S3C). Interestingly, Treg numbers were only significantly increased in WT ILC2 recipient mice (Figure 6E), whereas the Th1 cells were upregulated only in IL-4/13$^{-/-}$ ILC2 recipient mice and Th2, Th17 remained unchanged in both (Figure 6F). Furthermore, we investigated the potential therapeutic effect of ILC2 adoptive transfers (either from WT or IL-4/13$^{-/-}$ donor mice) by transferring ILC2s during established disease 4 days after the induction of SIA (Figure 6G). In line with our hypothesis that IL-4/13 play an important role in the initiation phase of SIA, we did not observe any clinical improvement in the later stages of the disease. Together, these data show the critical involvement of ILC2-derived cytokines IL-4/13 in the initiation phase of arthritis.

IL-4/13-Competent ILC2s Suppress Pathogenic RA Cytokines IL-1β and TNFα

On the basis of the reduced IL-1β and TNFα serum cytokine levels after ILC2 transfers, we further investigated the potential of ILC2s to affect IL-1β and TNFα cytokine secretion *in vitro*.

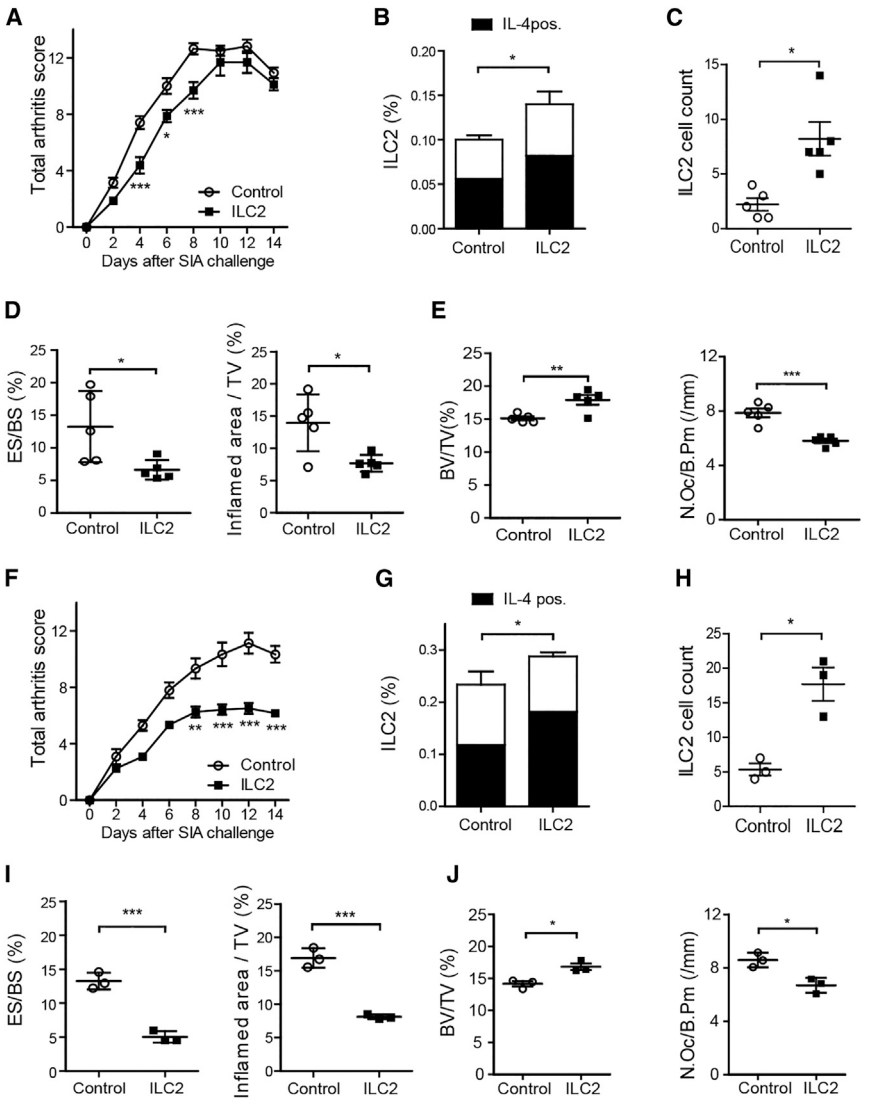

Figure 5. Adoptive Transfer of ILC2s Attenuates Arthritis

(A–J) Adoptive transfer of *ex vivo* expanded ILC2s into WT (n = 5) (A–E) and IL-7R$^{-/-}$ mice (n = 5) (F–J). The samples were obtained at day 14 after induction of SIA.

(A and F) Arthritis scores in control and ILC2 adoptive transferred mice.

(B and G) Flow cytometry analysis of total and IL-4^{+} ILC2s in the spleen. ILC2s were identified as lineage-negative (CD3e, CD4, CD8a, CD19, CD11b, and CD161) CD45^{+}, CD90.2^{+}, ST2^{+}, KLRG1^{+}, GATA3^{+} cells. (C and H) Immunohistochemical analysis of ILC2s in paws.

(D and I) Histomorphological analysis of paws showing eroded surface per bone surface (ES/BS) and inflamed area per total volume (TV).

(E and J) Systemic bone volume per tissue volume (BV/TV) and osteoclast number per bone perimeter (OcN/B.Pm) in the tibias of respective mice.

Representative data are from one of three (WT recipient mice) or two (IL-7R$^{-/-}$ recipient mice) independent experiments. Data are expressed as mean ± SEM. *p < 0.05, **p < 0.01, and ***p < 0.001.

Therefore, bone marrow-derived macrophages (BMDMs) were stimulated with lipopolysaccharide (LPS) ± additional ATP in the presence or absence of ILC2s from WT or IL-4/13$^{-/-}$ mice. As shown in Figure 7A, WT ILC2s significantly suppressed IL-1β secretion. This was dependent on IL-4/13, as IL-4/13$^{-/-}$ ILC2s were lacking this suppressive effect (Figure 7A). Although significant, the effect on TNFα (Figure 7B) was only mild, and no effect on IL-6 cytokine concentrations was observed (Figure 7C). These results show that ILC-derived IL-4/13 is capable of blocking IL-1β, a key effector cytokine in SIA (Ji et al., 2002) secreted by macrophages, which are the essential effector cells in SIA (Misharin et al., 2014).

DISCUSSION

Recent studies have elucidated the role of ILCs in inflammatory diseases, demonstrating their multi-functionality in disease exacerbation and prevention. For instance, ILC1 protect mice against *Toxoplasma gondii* infection (Klose et al., 2014), but they were also linked to pathogenic mucosal inflammation (Bernink et al., 2013). Similarly, ILC3 were reported to fuel intestinal inflammation (Pearson et al., 2016) but at the same time have been shown to be involved in wound healing after skin injury (Li et al., 2016). Although ILC3 and potentially also ILC1 may indeed have pro-inflammatory properties in arthritis, particularly related to IL-17 and IL-22 production and their role in spondyloarthritis, the effect of ILC2s on arthritis seems to be substantially different. ILC2s play prominent roles in the expulsion of helminths (Fallon et al., 2006) and in type 2 immunopathology after allergen exposure in the lungs (Halim et al., 2012). Importantly, type 2 immune responses have previously shown to exert regulatory effects on arthritis (Chen et al., 2016). Recently, Rauber et al. (2017) identified IL-9 as one regulator for the resolution of arthritis by showing that IL-9-secreting ILC2s restore the suppressive capacity of Tregs, enabling them to dampen already established chronic inflammations. In this study, we report on the fast and early increase in IL-4/13^{+} ILC2s and demonstrate their importance on the initiation phase of arthritis rather than the resolution of established chronic inflammatory arthritis. We can show that IL-4/13^{+} ILC2s are beneficial in the early initiation phase.

ILC2s rapidly increased after induction of arthritis and could be detected in the synovial tissue of two different arthritis models (SIA and CIA) as well as in human RA patients. Functional experiments revealed that genetically decreased ILC2 numbers in *Rora*^{cre}*Gata3*$^{fl/fl}$ or *Tie2*^{cre}/*ROR*α$^{fl/fl}$ mice exacerbated arthritis,

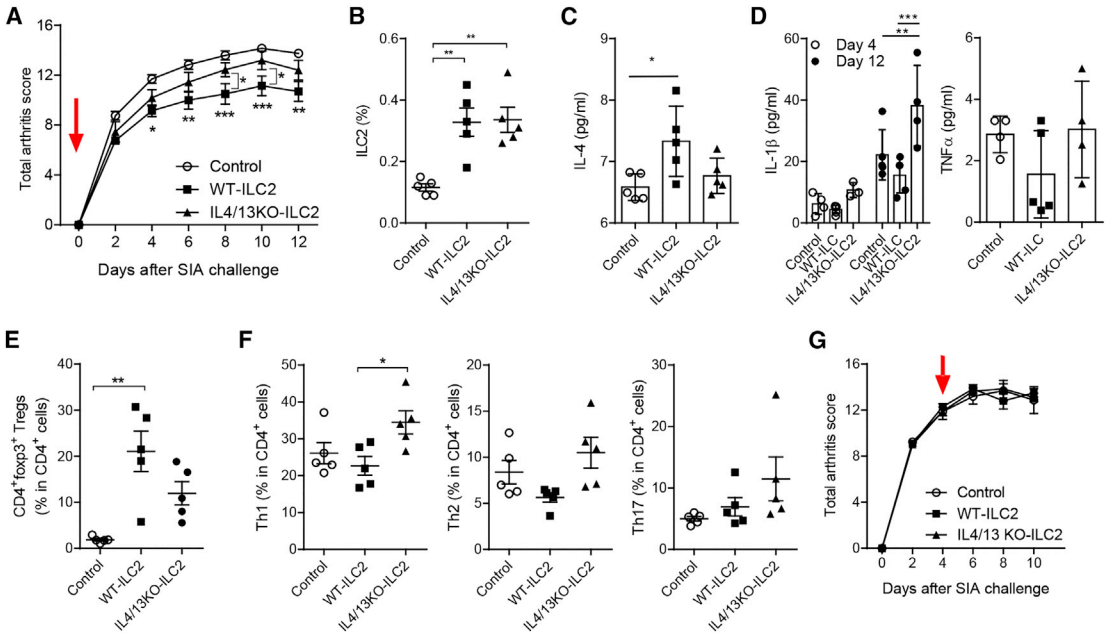

Figure 6. IL-4/13-Competent ILC2s Regulate Initiation of Arthritis

Adoptive transfer of *ex vivo* expanded WT or IL-4/13$^{-/-}$ ILC2s into WT recipient mice on day 0 before SIA was induced (n = 5). The samples were obtained at day 12 after SIA induction.

(A) Arthritis scores in control and ILC2 adoptive transferred mice. Red arrow indicates the transfer of ILC2s.

(B) Flow cytometry analysis of ILC2s in the spleen. ILC2s were identified as lineage-negative (CD3e, CD4, CD8a, CD19, CD11b, and CD161) CD45$^+$, CD90.2$^+$, ST2$^+$, KLRG1$^+$, GATA3$^+$ cells.

(C and D) Cytokine serum levels for (C) IL-4, (D) IL1-β, and TNFα analyzed by ELISA.

(E and F) Flow cytometry of spleen cells for CD4$^+$foxp3$^+$Treg (E) and effector Th1/2/17 (F) cell numbers. Adoptive transfer of *ex vivo* expanded WT and IL-4/13$^{-/-}$ ILC2s into WT mice at day 4 post-SIA induction (n = 5). (G) Arthritis scores in control and ILC2 adoptive transferred mice. ILC2s were transferred 4 days after the induction of SIA. Red arrow indicates the transfer of ILC2s.

Representative data are from one of two independent experiments. Data are expressed mean ± SEM. *p < 0.05, **p < 0.01, and ***p < 0.001.

while *in vivo* gain-of-function models, such as IL-25/33 mc or IL2c treatment, consistently attenuated arthritis and mitigated bone destruction. Although IL-25/33 mc and IL2c treatments both provide strong support for ILC2s being regulatory cellular mediators in arthritis, additional effects not directly based on ILC2s cannot be excluded. For instance, it was shown that IL2c enhances Arg1 expression (Pelly et al., 2016), IL-25 induces Th2 responses (Fort et al., 2001), and IL-33 increases Treg frequency (Biton et al., 2016; Schiering et al., 2014), upregulates FcgRIIB expression on macrophages (Anthony et al., 2011), and suppresses osteoclast numbers (Zaiss et al., 2011). Of note, recently it was shown that IL-33 is important for the egress of ILC2s from the bone marrow, further supporting our attenuating effects of IL-25/33 mc treatment on arthritis scores (Stier et al., 2018). Also, differences of ILC2s in the capacity to induce Tregs might evolve of diverse stimuli used to *in vivo* increase ILC2 numbers compared with adoptive transfers of mature, *ex vivo* pre-activated ILC2s. To exclude non-ILC2-mediated effects of IL-25/33 mc and IL2c treatments, we performed adoptive transfer experiments of sorted ILC2s and found that these cells directly attenuated arthritis scores. This effect was dependent on the capacity of ILC2 to secret IL-4/13, as IL4/13$^{-/-}$ ILC2s failed to attenuate arthritis. IL-4/13$^+$ ILC2s were critical during the initiation phase of arthritis, as adoptive transfer of ILC2 at later time points failed to affect arthritis. Beside the prominent downregulation of IL-1β by IL-4/13$^+$ ILC2s, which is a key effector cytokine in arthritis (Ji et al., 2002; Lamacchia et al., 2012), IL-4 itself acts as a regulatory cytokine in arthritis, as it fosters Th2 cell commitment, induces Ig class switching to the Th2-associated isotypes IgG1 and IgE (Nelms et al., 1999), and has the ability to suppress synoviocyte proliferation (Dechanet et al., 1993). In accordance, most (Horsfall et al., 1997; Joosten et al., 1997; Myers et al., 2002) but not all (Ohmura et al., 2005) studies showed that IL-4 has attenuating effects on arthritis. Studies of IL-13 and arthritis are limited, and although IL-13 is found in RA (Liu et al., 2016; Siloşi et al., 2016; Tokayer et al., 2002), only one study addressed its functional role by showing that IL-25/IL-13 has an attenuating effect on arthritis (Liu et al., 2016; Siloşi et al., 2016; Tokayer et al., 2002). Taken together these previous works and our findings suggest that a key regulatory factor in arthritis is the generation of IL-4/13-competent ILC2s.

In summary, we identified ILC2s as a regulatory cell lineage in the early development of arthritis. Enhancement of ILC2 numbers may therefore be a method to effectively block the development of this severe inflammatory joint disease.

EXPERIMENTAL PROCEDURES

Mice

C57BL/6J mice as well as DBA/1 and BALB/cJRj mice were purchased from The Jackson Laboratory and were acclimated for 1 week, followed by a

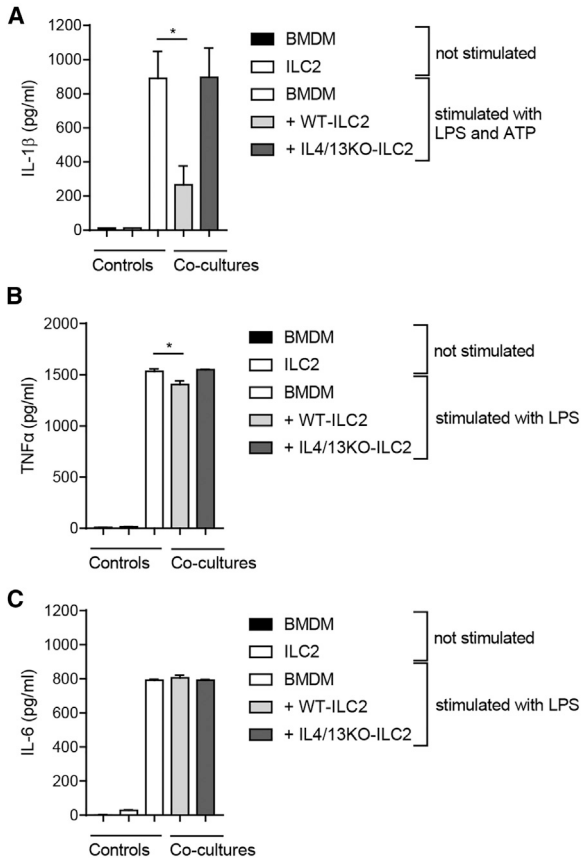

Figure 7. IL-4/-13-Competent ILC2s Suppress IL-1β Secretion in Macrophages

WT or IL-4/13$^{-/-}$ ILC2s were co-cultured with bone marrow-derived macrophages (BMDMs) *in vitro* with 60,000 BMDMs and 30,000 ILC2/well. The supernatant was analyzed after 6 hr stimulation with LPS (0.1 ng/μL) ± ATP (5 mM).

(A–C) IL-1β (A), TNFα (B), and IL-6 (C) measured by ELISA in the culture supernatants.

Representative data are from one of two independent experiments. Data are expressed as mean ± SEM. *p < 0.05.

2 week co-housing period before the experiments started. B6-Ptprca-Pep3b/BoyJ Il7rtm1Imx/J (IL-7R$^{-/-}$) mice were kindly provided by Immo Prinz from Medizinische Hochschule (Hannover, Germany). BALB/cJRj IL-4/13-knockout mice were kindly provided by David Vöhringer, Department of Infection Biology, Institute for Medical Microbiology, Immunology and Hygiene, Friedrich-Alexander University Erlangen-Nürnberg (Erlangen, Germany) (Turqueti-Neves et al., 2015). *Rora*^{cre}*Gata3*$^{fl/fl}$ mice and Tie2^{Cre}*Rora* $^{fl/fl}$ mice were kindly provided by Stefan Wirtz, Department of Internal Medicine 1, University of Erlangen-Nürnberg (Erlangen, Germany). All mice were maintained under specific pathogen-free conditions at Präklinisches Experimentelles Tierzentrum (PETZ) (Erlangen, Germany). The local ethics committee of the government of Mittelfranken approved all experiments.

Experimental Model of Arthritis

For CIA, arthritis was induced in 8-week-old female DBA/1J mice by subcutaneous (s.c.) injection at the base of the tail with 100 μL. Mice were re-challenged after 21 days by intradermal immunization in the base of the tail with 0.25 mg bovine type II collagen (CII; ChondrexRedmond, WA) in complete Freund's adjuvant (CFA; Difco Laboratory), containing 2.5 mg/mL killed *Mycobacterium tuberculosis* (H37Ra). The paws were evaluated for joint swelling three times per week. Each paw was individually scored using a 5-point scale: 0 = normal paw, 1 = minimal swelling or redness, 2 = redness and swelling involving the entire forepaw, 3 = redness and swelling involving the entire limp, and 4 = joint deformity or ankylosis or both. Paw width was measured using calipers. Likewise, serum-induced arthritis (SIA) was induced in 8-week-old female C57BL/6 mice by intraperitoneal (i.p.) injection of 150 μL pooled K/BxN serum. The paws were evaluated for joint swelling three times per week, the same as for CIA. Each paw was individually scored using the same scales as for CIA. For *in vivo* treatment with mc vectors, 8-week-old female C57BL/6 mice and BALB/cJRj were treated with 4 μg of mc vector of IL-25 and IL-33 hydrodynamically 5 days before the initiation of arthritis (SIA), as described previously (Liu et al., 1999). For *in vivo* treatments with IL-2 complex, 8-week-old C57BL/6 female mice were treated with IL-2 complex (IL2c) formed of recombinant IL-2 (R&D, Abingdon, UK) and anti-IL-2 antibody (clone JES6-1A12; BioXcell, West Lebanon, NH). These materials were prepared at a 1:10 ratio of IL-2 to anti-IL-2 (2.5 μg:25 μg) in sterile PBS for i.p. delivery, as described previously (Pelly et al., 2016). Mice were challenged with two i.p. doses of IL2c on days −7 and 0 before SIA was initiated.

Human Study Subjects

Peripheral blood from RA patients (n = 59) and healthy controls (n = 21) was analyzed using flow cytometry for ILC2s and their demographic and disease activity by disease activity score 28 (DAS28)-ESR, in which we counted the number of tender joints and swollen joints and recorded general health scale by patient for themselves and measured erythrocyte sedimentation rate (ESR) in blood. The samples of synovial tissues were obtained from patients with active RA using needle arthroscopy. All analyses of human material were performed in full agreement with institutional guidelines and with the approval of the ethics committee of the University Hospital Erlangen. Informed consent and permission to use the obtained data for research were obtained from all subjects enrolled in the study.

Flow Cytometry

For detection of ILC2s in human blood samples, cells were stained with biotinylated CD11c (337232; BioLegend), CD123 (306004; BioLegend), CD14 (367106; BioLegend), CD34 (343524; BioLegend), FcdR1 (13-5899-82; eBioscience), TCRαβ (306704; BioLegend), TCRγδ (331206; BioLegend), CD303 (orb114050; Biobyt), and CD94 (130-098-966; Miltenyi Biotec), followed by streptavidin-labeled Texas red (562318; BD Bioscience) and CD3 (300322; BioLegend), CD127 (351312; BioLegend), CD161 (339942; BioLegend), CRTH (350118; BioLegend), and GATA3 (653804; BioLegend) (Figure S5A). For detection of ILC2s in mice, cell suspensions from blood, spleen, mesenteric lymph nodes, and lung were stained with biotinylated CD3e (100304; BioLegend), CD4 (100508; BioLegend), CD8a (100704; BioLegend), CD19 (115504; BioLegend), CD11b (101204; BioLegend), and CD161 (108704; BioLegend) followed by streptavidin-labeled Texas red (562318; BD Bioscience) and CD45 (103108; BioLegend), CD90.2 (140322; BioLegend), KLRG1 (138426; BioLegend), ST2 (101001PE; MD Bioscience), and GATA3 (653806; BioLegend). Prior to staining with antibodies (Abs), a LIVE/DEAD Fixable Violet Dead Cell Stain Kit (Life Technologies) was used to exclude dead cells. For intracellular cytokine staining of ILC2s, total lymphocytes were incubated *in vitro* overnight with GATA3 AB. ILC2s were gated on CD45$^+$ Lin$^-$ ST2$^+$ KLRG1$^+$ CD90.2$^+$ GATA3$^+$ LIVE/DEAD Violet single cells (Figure S5B). All flow cytometry analyses were performed using the CytoFLEX Platform (Beckman Coulter) and analyzed using Kaluza analysis-software (Beckman Coulter). For ILC2 cell sorting, a MoFlo Astrios EQ cell sorter (Beckman Coulter) was used to purify ILC2s (Figure S5D). Cells from spleen were stained with CD3 (130-192-294; Miltenyi Biotec), CD5 (100606; BioLegend), B220 (11-0452-82; eBioscience), NKp46 (137618; BioLegend), CD11b (17-0112-82; eBioscience), CD11c (17-0114-82; eBioscience), KLRG1 (138426; BioLegend), ICOS (564070; BD Bioscience), and ST2 (101001PE; MD Bioscience). ILC2s were identified as CD5$^-$ B220$^-$ CD45R$^-$ NKp46$^-$ CD11b$^-$ CD11c$^-$ ICOS$^+$ KLRG1$^+$ ST2$^+$ cells. The purity of ILC2 populations was 95%, as verified by post-sort flow cytometric analysis.

Cell Cultures

For cell culture, ILC2s were cultured in DMEM high glucose (Life Technologies) containing 10% fetal calf serum (FCS), 1% penicillin-streptomycin solution

(HyClone), 50 μM 2-mercaptoethanol, 1 mM sodium pyruvate (Life Technologies), non-essential amino acids (Life Technologies), and 20 mM HEPES (pH 7.4), plus various stimulants. Sorted ILC2s from the spleens of mice treated with mcIL-25 and mcIL-33 were stimulated with 50 ng/mL of IL-2, IL-7, IL-25, and IL-33 and 20 ng/mL TSLP to activate and expand ILC2s for 14 days before flow cytometric analysis or adoptive transfer experiments, as previously described (Duerr et al., 2016). Before the experiments, the expanded cells were analyzed using FACS again (Figure S5E). For BMDM co-cultures with ILC2s, hematopoietic bone marrow cells were purified from tibial bone with a 70 μm cell strainer, cultured overnight, and stimulated with appropriate growth medium (MEM Alpha Medium 1× GlutaMAX, 32571-028 [Gibco], containing 10% L929 conditioned medium, 10% FCS, and 1% penicillin/streptomycin) at 37°C with 5% CO_2. To obtain BMDMs, bone marrow cells were incubated with growth medium (MEM Alpha Medium 1× GlutaMAX, containing 10% L929 conditioned medium, 10% FCS, and 1% penicillin/streptomycin) for 4 days and then seeded for experiments. BMDMs were seeded 60,000 cells/well in a 96-well plate. Thirty thousand ILC2s were seeded with BMDMs. The supernatant were collected after stimulation with LPS (0.1 ng/μL) ± ATP (5 mM) and were analyzed using ELISA.

Measurement of Cytokine Expression

For measurement of the expression of IL-1β, IL-6, IL-25, IL-33, and TNFα, ELISA kits from Invitrogen Thermo Fisher Scientific were used. To analyze expression of Th serum cytokines, we used LEGENDplex (BioLegend) according to the manufacturer's instructions. For measurement of IL-4 (562915; BioLegend) (Figure S5C), IL-5 (504311; BioLegend), and IL-13 (25-5941-82; eBioscience) expression on ILC2s by FACS, splenocytes were incubated for 4 hr with PMA (50 ng/mL) and ionomycin (1 μg/mL).

Adoptive Transfer Experiment

For ILC2 cell adoptive transfer, donor mice were hydrodynamically injected with 4 μg of IL-25 mc and IL-33 mc for induction of ILC2s. Five days after plasmid injection, flow cytometry-purified donor splenic ILC2s were expanded *in vitro* (see Cell Cultures) before 1 × 10^6 cells intravenous (i.v.) injection into C57BL/6 or BALB/cJRj mice. ILC2s were analyzed in the splenocytes of recipient mice post-ILC2 cell transfer. To examine the presence of ILC2s in the joints, we generated bone marrow chimeras. We isolated bone marrow from *Rora*^{cre} *TdTomato*$^{fl/fl}$ mice and transferred 1 × 10^6 cells of femoral and tibial bone marrow monocytes (BMMs) into irradiated naive C57BL/6 mice (10 Gy). Eight weeks after the transfer of BMMs, 150 μL serum of K/BxN mice was injected to initiate arthritis. Mice were sacrificed 8 days later, and tibial bones and paws were analyzed histologically.

Histology

For histological analysis, tarsal joints of hind paws and tibial bones were fixed in 4% formalin for 12 hr and decalcified in EDTA (Sigma-Aldrich). Serial paraffin sections (2 μm) were stained for H&E and tartrate-resistant acid phosphatase (TRAP) using a Leukocyte Acid Phosphatase Kit (Sigma-Aldrich) according to the manufacturer's instructions. Inflammation, bone destruction, and osteoclast numbers were quantified using a microscope (Nikon) equipped with a digital camera and an image analysis system for performing histomorphometry (Osteomeasure; OsteoMetrics). For histological analysis in bone marrow chimera experiment using *Rora*^{cre} *TdTomato*$^{fl/fl}$ mice, we stained ILC2s using Abs against IL-17RB (sc11754; Santa Cruz), CD3ε (17-0031; eBioscience), and DAPI. For other histological analyses, we stained ILC2s using Abs against IL17RB, ST2 (3363; ProSci), CD3ε, CD11b (1124; R&D Systems), CD11c (ab33483; Abcam), B220 (14-0452; eBioscience), Ly6G (MAB1037; R&D Systems), and DAPI.

Statistical Analysis

Statistical analyses were performed using Student's t test, the Mann-Whitney test, and one-way or two-way ANOVA followed by Tukey's multiple-comparison post-test. For all experiments, p values are indicated as *$p < 0.05$, **$p < 0.01$, or ***$p < 0.001$. Graph generation and statistical analyses were performed using Prism version 6c software (GraphPad).

SUPPLEMENTAL INFORMATION

Supplemental Information includes five figures and can be found with this article online at https://doi.org/10.1016/j.celrep.2018.06.005.

ACKNOWLEDGMENTS

This study was supported by the Deutsche Forschungsgemeinschaft priority program (SPP, ZA899/4-1) 1937 Innate Lymphoid Cells, 1468 IMMUNOBONE, and CRC1181, Bundesministerium für Bildung und Forschung (BMBF; project METARTHROS), the TEAM project of the European Union, and the Innovative Medicines Initiative (IMI)-funded project BTCure. We are grateful to Prof. Immo Prinz (Medizinische Hochschule, Hannover, Germany) for kindly providing B6-Ptprca-Pep3b/BoyJ Il7rtm1Imx/J (IL-7R$^{-/-}$) mice, Prof. David Voehringer (Department of Infection Biology, Institute for Medical Microbiology, Immunology and Hygiene, Friedrich-Alexander University Erlangen-Nuremberg, Erlangen, Germany) for kindly providing BALB/cJRj IL-4/-13-knockout mice, and Dr. Stefan Wirtz (Department of Internal Medicine 1, University of Erlangen-Nuremberg, Erlangen, Germany) for kindly providing *Rora*^{cre}*Gata3*$^{fl/fl}$ mice and Tie2^{Cre}*Rora*^{flox} mice. We thank Uwe Appelt and Markus Mroz (Core Unit, Cell Sorting and Immunomonitoring, Friedrich-Alexander-University Erlangen-Nürnberg and Universitätsklinikum Erlangen, Erlangen, Germany) for cell sorting. We also thank Margarete Schimpf, Barbara Happich and Viktoria Lebed for technical support.

AUTHOR CONTRIBUTIONS

Y.O., G.S., and M.M.Z. conceived and designed the study. Y.O., M.F., T.P., S.L., D.A., C.S., K.S., A.R., and M.K. performed the experiments. Y.O., N.Y., D.L.B., A.B., G.K., S.W., N.A., T.K., and M.M.Z. analyzed data. Y.O., K.S., and M.M.Z. wrote the manuscript.

DECLARATION OF INTERESTS

The authors declare no competing interests.

Received: August 15, 2017
Revised: May 3, 2018
Accepted: June 1, 2018
Published: July 3, 2018

REFERENCES

Anthony, R.M., Kobayashi, T., Wermeling, F., and Ravetch, J.V. (2011). Intravenous gammaglobulin suppresses inflammation through a novel T(H)2 pathway. Nature *475*, 110–113.

Bernink, J.H., Peters, C.P., Munneke, M., te Velde, A.A., Meijer, S.L., Weijer, K., Hreggvidsdottir, H.S., Heinsbroek, S.E., Legrand, N., Buskens, C.J., et al. (2013). Human type 1 innate lymphoid cells accumulate in inflamed mucosal tissues. Nat. Immunol. *14*, 221–229.

Biton, J., Khaleghparast Athari, S., Thiolat, A., Santinon, F., Lemeiter, D., Hervé, R., Delavallée, L., Levescot, A., Roga, S., Decker, P., et al. (2016). In vivo expansion of activated Foxp3+ regulatory T cells and establishment of a type 2 immune response upon IL-33 treatment protect against experimental arthritis. J. Immunol. *197*, 1708–1719.

Chen, Z., Andreev, D., Oeser, K., Krljanac, B., Hueber, A., Kleyer, A., Voehringer, D., Schett, G., and Bozec, A. (2016). Th2 and eosinophil responses suppress inflammatory arthritis. Nat. Commun. *7*, 11596.

Ciccia, F., Accardo-Palumbo, A., Alessandro, R., Rizzo, A., Principe, S., Peralta, S., Raiata, F., Giardina, A., De Leo, G., and Triolo, G. (2012). Interleukin-22 and interleukin-22-producing NKp44+ natural killer cells in subclinical gut inflammation in ankylosing spondylitis. Arthritis Rheum. *64*, 1869–1878.

Ciccia, F., Guggino, G., Rizzo, A., Saieva, L., Peralta, S., Giardina, A., Cannizzaro, A., Sireci, G., De Leo, G., Alessandro, R., and Triolo, G. (2015). Type 3 innate lymphoid cells producing IL-17 and IL-22 are expanded in the gut,

in the peripheral blood, synovial fluid and bone marrow of patients with ankylosing spondylitis. Ann. Rheum. Dis. *74*, 1739–1747.

Cuthbert, R.J., Fragkakis, E.M., Dunsmuir, R., Li, Z., Coles, M., Marzo-Ortega, H., Giannoudis, P., Jones, E., El-Sherbiny, Y.M., and McGonagle, D. (2017). Brief report: human enthesis group 3 innate lymphoid cells. Arthritis Rheumatol. *69*, 1816–1822.

Dalbeth, N., and Callan, M.F. (2002). A subset of natural killer cells is greatly expanded within inflamed joints. Arthritis Rheum. *46*, 1763–1772.

Dechanet, J., Briolay, J., Rissoan, M.C., Chomarat, P., Galizzi, J.P., Banchereau, J., and Miossec, P. (1993). IL-4 inhibits growth factor-stimulated rheumatoid synoviocyte proliferation by blocking the early phases of the cell cycle. J. Immunol. *151*, 4908–4917.

Duerr, C.U., McCarthy, C.D., Mindt, B.C., Rubio, M., Meli, A.P., Pothlichet, J., Eva, M.M., Gauchat, J.F., Qureshi, S.T., Mazer, B.D., et al. (2016). Type I interferon restricts type 2 immunopathology through the regulation of group 2 innate lymphoid cells. Nat. Immunol. *17*, 65–75.

Fallon, P.G., Ballantyne, S.J., Mangan, N.E., Barlow, J.L., Dasvarma, A., Hewett, D.R., McIlgorm, A., Jolin, H.E., and McKenzie, A.N. (2006). Identification of an interleukin (IL)-25-dependent cell population that provides IL-4, IL-5, and IL-13 at the onset of helminth expulsion. J. Exp. Med. *203*, 1105–1116.

Fort, M.M., Cheung, J., Yen, D., Li, J., Zurawski, S.M., Lo, S., Menon, S., Clifford, T., Hunte, B., Lesley, R., et al. (2001). IL-25 induces IL-4, IL-5, and IL-13 and Th2-associated pathologies in vivo. Immunity *15*, 985–995.

Gause, W.C., Wynn, T.A., and Allen, J.E. (2013). Type 2 immunity and wound healing: evolutionary refinement of adaptive immunity by helminths. Nat. Rev. Immunol. *13*, 607–614.

Halim, T.Y., Krauss, R.H., Sun, A.C., and Takei, F. (2012). Lung natural helper cells are a critical source of Th2 cell-type cytokines in protease allergen-induced airway inflammation. Immunity *36*, 451–463.

Horsfall, A.C., Butler, D.M., Marinova, L., Warden, P.J., Williams, R.O., Maini, R.N., and Feldmann, M. (1997). Suppression of collagen-induced arthritis by continuous administration of IL-4. J. Immunol. *159*, 5687–5696.

Ji, H., Pettit, A., Ohmura, K., Ortiz-Lopez, A., Duchatelle, V., Degott, C., Gravallese, E., Mathis, D., and Benoist, C. (2002). Critical roles for interleukin 1 and tumor necrosis factor alpha in antibody-induced arthritis. J. Exp. Med. *196*, 77–85.

Joosten, L.A., Lubberts, E., Durez, P., Helsen, M.M., Jacobs, M.J., Goldman, M., and van den Berg, W.B. (1997). Role of interleukin-4 and interleukin-10 in murine collagen-induced arthritis. Protective effect of interleukin-4 and interleukin-10 treatment on cartilage destruction. Arthritis Rheum. *40*, 249–260.

Klose, C.S.N., Flach, M., Möhle, L., Rogell, L., Hoyler, T., Ebert, K., Fabiunke, C., Pfeifer, D., Sexl, V., Fonseca-Pereira, D., et al. (2014). Differentiation of type 1 ILCs from a common progenitor to all helper-like innate lymphoid cell lineages. Cell *157*, 340–356.

Koo, J., Kim, S., Jung, W.J., Lee, Y.E., Song, G.G., Kim, K.S., and Kim, M.Y. (2013). Increased lymphocyte infiltration in rheumatoid arthritis is correlated with an increase in LTi-like cells in synovial fluid. Immune Netw. *13*, 240–248.

Lamacchia, C., Rodriguez, E., Palmer, G., Vesin, C., Seemayer, C.A., Rubbia-Brandt, L., and Gabay, C. (2012). Mice deficient in hepatocyte-specific IL-1Ra show delayed resolution of concanavalin A-induced hepatitis. Eur. J. Immunol. *42*, 1294–1303.

Leijten, E.F., van Kempen, T.S., Boes, M., Michels-van Amelsfort, J.M., Hijnen, D., Hartgring, S.A., van Roon, J.A., Wenink, M.H., and Radstake, T.R. (2015). Brief report: enrichment of activated group 3 innate lymphoid cells in psoriatic arthritis synovial fluid. Arthritis Rheumatol. *67*, 2673–2678.

Li, Z., Hodgkinson, T., Gothard, E.J., Boroumand, S., Lamb, R., Cummins, I., Narang, P., Sawtell, A., Coles, J., Leonov, G., et al. (2016). Epidermal Notch1 recruits RORγ(+) group 3 innate lymphoid cells to orchestrate normal skin repair. Nat. Commun. *7*, 11394.

Liu, F., Song, Y., and Liu, D. (1999). Hydrodynamics-based transfection in animals by systemic administration of plasmid DNA. Gene Ther. *6*, 1258–1266.

Liu, D., Cao, T., Wang, N., Liu, C., Ma, N., Tu, R., and Min, X. (2016). IL-25 attenuates rheumatoid arthritis through suppression of Th17 immune responses in an IL-13-dependent manner. Sci. Rep. *6*, 36002.

McHedlidze, T., Waldner, M., Zopf, S., Walker, J., Rankin, A.L., Schuchmann, M., Voehringer, D., McKenzie, A.N., Neurath, M.F., Pflanz, S., and Wirtz, S. (2013). Interleukin-33-dependent innate lymphoid cells mediate hepatic fibrosis. Immunity *39*, 357–371.

Misharin, A.V., Cuda, C.M., Saber, R., Turner, J.D., Gierut, A.K., Haines, G.K., 3rd, Berdnikovs, S., Filer, A., Clark, A.R., Buckley, C.D., et al. (2014). Nonclassical Ly6C(-) monocytes drive the development of inflammatory arthritis in mice. Cell Rep. *9*, 591–604.

Mjösberg, J., Bernink, J., Golebski, K., Karrich, J.J., Peters, C.P., Blom, B., te Velde, A.A., Fokkens, W.J., van Drunen, C.M., and Spits, H. (2012). The transcription factor GATA3 is essential for the function of human type 2 innate lymphoid cells. Immunity *37*, 649–659.

Moro, K., Yamada, T., Tanabe, M., Takeuchi, T., Ikawa, T., Kawamoto, H., Furusawa, J., Ohtani, M., Fujii, H., and Koyasu, S. (2010). Innate production of T(H)2 cytokines by adipose tissue-associated c-Kit(+)Sca-1(+) lymphoid cells. Nature *463*, 540–544.

Myers, L.K., Tang, B., Stuart, J.M., and Kang, A.H. (2002). The role of IL-4 in regulation of murine collagen-induced arthritis. Clin. Immunol. *102*, 185–191.

Neill, D.R., Wong, S.H., Bellosi, A., Flynn, R.J., Daly, M., Langford, T.K., Bucks, C., Kane, C.M., Fallon, P.G., Pannell, R., et al. (2010). Nuocytes represent a new innate effector leukocyte that mediates type-2 immunity. Nature *464*, 1367–1370.

Nelms, K., Keegan, A.D., Zamorano, J., Ryan, J.J., and Paul, W.E. (1999). The IL-4 receptor: signaling mechanisms and biologic functions. Annu. Rev. Immunol. *17*, 701–738.

Ohmura, K., Nguyen, L.T., Locksley, R.M., Mathis, D., and Benoist, C. (2005). Interleukin-4 can be a key positive regulator of inflammatory arthritis. Arthritis Rheum. *52*, 1866–1875.

Pearson, C., Thornton, E.E., McKenzie, B., Schaupp, A.L., Huskens, N., Griseri, T., West, N., Tung, S., Seddon, B.P., Uhlig, H.H., and Powrie, F. (2016). ILC3 GM-CSF production and mobilisation orchestrate acute intestinal inflammation. eLife *5*, e10066.

Pelly, V.S., Kannan, Y., Coomes, S.M., Entwistle, L.J., Rückerl, D., Seddon, B., MacDonald, A.S., McKenzie, A., and Wilson, M.S. (2016). IL-4-producing ILC2s are required for the differentiation of T_H2 cells following Heligmosomoides polygyrus infection. Mucosal Immunol. *9*, 1407–1417.

Rauber, S., Luber, M., Weber, S., Maul, L., Soare, A., Wohlfahrt, T., Lin, N.Y., Dietel, K., Bozec, A., Herrmann, M., et al. (2017). Resolution of inflammation by interleukin-9-producing type 2 innate lymphoid cells. Nat. Med. *23*, 938–944.

Ren, J., Feng, Z., Lv, Z., Chen, X., and Li, J. (2011). Natural killer-22 cells in the synovial fluid of patients with rheumatoid arthritis are an innate source of interleukin 22 and tumor necrosis factor-α. J. Rheumatol. *38*, 2112–2118.

Robinette, M.L., Bando, J.K., Song, W., Ulland, T.K., Gilfillan, S., and Colonna, M. (2017). IL-15 sustains IL-7R-independent ILC2 and ILC3 development. Nat. Commun. *8*, 14601.

Rodríguez-Carrio, J., Hähnlein, J.S., Ramwadhdoebe, T.H., Semmelink, J.F., Choi, I.Y., van Lienden, K.P., Maas, M., Gerlag, D.M., Tak, P.P., Geijtenbeek, T.B., and van Baarsen, L.G. (2017). Brief report: altered innate lymphoid cell subsets in human lymph node biopsy specimens obtained during the at-risk and earliest phases of rheumatoid arthritis. Arthritis Rheumatol. *69*, 70–76.

Salimi, M., Barlow, J.L., Saunders, S.P., Xue, L., Gutowska-Owsiak, D., Wang, X., Huang, L.C., Johnson, D., Scanlon, S.T., McKenzie, A.N., et al. (2013). A role for IL-25 and IL-33-driven type-2 innate lymphoid cells in atopic dermatitis. J. Exp. Med. *210*, 2939–2950.

Schiering, C., Krausgruber, T., Chomka, A., Fröhlich, A., Adelmann, K., Wohlfert, E.A., Pott, J., Griseri, T., Bollrath, J., Hegazy, A.N., et al. (2014). The alarmin IL-33 promotes regulatory T-cell function in the intestine. Nature *513*, 564–568.

Siloşi, I., Boldeanu, M.V., Cojocaru, M., Biciuşcă, V., Pădureanu, V., Bogdan, M., Badea, R.G., Avramescu, C., Petrescu, I.O., Petrescu, F., and Siloşi, C.A. (2016). The relationship of cytokines IL-13 and IL-17 with autoantibodies profile in early rheumatoid arthritis. J. Immunol. Res. *2016*, 3109135.

Stier, M.T., Zhang, J., Goleniewska, K., Cephus, J.Y., Rusznak, M., Wu, L., Van Kaer, L., Zhou, B., Newcomb, D.C., and Peebles, R.S., Jr. (2018). IL-33 promotes the egress of group 2 innate lymphoid cells from the bone marrow. J. Exp. Med. *215*, 263–281.

Tokayer, A., Carsons, S.E., Chokshi, B., and Santiago-Schwarz, F. (2002). High levels of interleukin 13 in rheumatoid arthritis sera are modulated by tumor necrosis factor antagonist therapy: association with dendritic cell growth activity. J. Rheumatol. *29*, 454–461.

Turqueti-Neves, A., Otte, M., Schwartz, C., Schmitt, M.E., Lindner, C., Pabst, O., Yu, P., and Voehringer, D. (2015). The extracellular domains of IgG1 and T cell-derived IL-4/IL-13 are critical for the polyclonal memory IgE response in vivo. PLoS Biol. *13*, e1002290.

Vonarbourg, C., and Diefenbach, A. (2012). Multifaceted roles of interleukin-7 signaling for the development and function of innate lymphoid cells. Semin. Immunol. *24*, 165–174.

Zaiss, M.M., Kurowska-Stolarska, M., Böhm, C., Gary, R., Scholtysek, C., Stolarski, B., Reilly, J., Kerr, S., Millar, N.L., Kamradt, T., et al. (2011). IL-33 shifts the balance from osteoclast to alternatively activated macrophage differentiation and protects from TNF-alpha-mediated bone loss. J. Immunol. *186*, 6097–6105.